Structure–Distribution Relationships for Metal-Labeled Myocardial Imaging Agents: Comparison of a Series of Cationic Gallium(III) Complexes with Hexadentate Bis(salicylaldimine) Ligands

Brenda W. Tsang, Carla J. Mathias, Phillip E. Fanwick, and Mark A. Green*

Departments of Medicinal Chemistry and Chemistry, Purdue University, West Lafayette, Indiana 47907-1333

Received February 28, 1994®

A series of 10 cationic gallium(III) complexes with hexadentate bis(salicylaldimine) ligands were synthesized, characterized, radiolabeled with ^{67}Ga, and screened in a rat model to assess their potential as ^{68}Ga radiopharmaceuticals for imaging the heart with positron emission tomography. The tris(salicylaldimine) ligand precursors were synthesized by condensation of either bis(3-aminopropyl)ethylenediamine (BAPEN) or bis(2,2-dimethyl-3-aminopropyl)ethylenediamine (DM-BAPEN) with 3 equiv of a salicylaldehyde derivative containing alkyl, alkoxy, or alkylamino substituents in the 4, 5, or 6 position of the aromatic ring. The cationic six-coordinate gallium(III) bis(salicylaldimine) complexes were obtained by reaction of these tris(salicylaldimines) with tris(acetylacetonato)gallium(III). X-ray crystallographic confirmation of the molecular structure of Ga[(4,6-(MeO)$_2$sal)$_2$DM-BAPEN]$^+$I$^-$ shows the Ga cation to adopt a pseudo-octahedral N_4O_2 coordination sphere with a *trans* configuration. All of the ^{67}Ga complexes are lipophilic with measured octanol/water partition coefficients (P) varying from log P = 0.84 to 3.00. These ^{67}Ga-labeled complexes are all found to exhibit significant myocardial uptake following intravenous administration to rats (ranging from 0.34 to 1.08% of the injected dose in myocardium at 1 min postinjection) combined with the desired myocardial retention of tracer.

Introduction

Positron emission tomography (PET) is a powerful medical imaging technique that allows quantitative evaluation of regional tissue physiology and biochemistry using radiopharmaceuticals labeled with radionuclides that decay by positron emission.[1] However, widespread clinical use of PET has been hampered by the expense associated with purchase and operation of the hospital-based cyclotron that is needed to produce the most commonly used positron-emitting nuclides (^{15}O, ^{13}N, ^{11}C, and ^{18}F). This financial obstacle to the use of PET could be avoided by the development of radiopharmaceuticals labeled with gallium-68, which is available from a long-lived parent/daughter generator system (^{68}Ge/^{68}Ga).[2] The 271 day half-life of the ^{68}Ge parent gives this generator a long shelf life, while the 68 min half-life of the ^{68}Ga daughter is sufficiently long to allow the synthesis of a wide variety of radiopharmaceuticals.[3-4] In addition, if the tracer kinetics of a ^{68}Ga radiopharmaceutical are such that the tracer is retained in target tissues, this 68 min half-life would allow the use of "long" image acquisition periods for reconstruction of high-resolution tomographic images with excellent counting statistics.

The determination of regional myocardial perfusion is an important clinical application of PET. Several ^{68}Ga compounds have been described in the literature for use as myocardial imaging agents. The neutral ^{68}Ga[(5-MeOsal)$_3$tame] and ^{68}Ga[(sal)$_3$tame-O-*i*-Bu] complexes and the cationic ^{68}Ga[BAT-TECH]$^+$ complex all exhibit significant myocardial uptake following intravenous administration to animals, with the latter two rapidly providing excellent heart-to-blood ratios.[5-7] Unfortunately, none of these compounds provide the myocardial retention of ^{68}Ga radioactivity that is needed to allow exploitation of the ^{68}Ga half-life through slow acquisition of high-count images.

Previous studies describing cationic and neutral ^{99m}Tc radiopharmaceuticals have demonstrated that, while lipophilic uncharged complexes often exhibit high myocardial uptake shortly after iv injection, they also are fairly rapidly cleared from myocardium when blood concentrations of tracer drop.[8] However, lipophilic monocationic complexes are frequently retained in the heart as long as they maintain their positive charge within the myocardium.[8-10]

We have recently reported a cationic ^{68}Ga complex with an $N_4O_2^{2-}$ Schiff base ligand that in animal models shows significant myocardial uptake and indefinite tracer retention in myocardium.[11] While this compound exhibits desirable properties, the net myocardial uptake of this particular derivative remains less than ideal. Consequently, we are investigating derivatization of the Ga[(4,6-(MeO)$_2$sal)$_2$BAPEN]$^+$ lead compound in an attempt to identify related compounds capable of providing improved myocardial uptake while maintaining the desired tracer retention in myocardium along with rapid clearance from background tissues (*e.g.*, blood and liver). We report here the results obtained with a series of 10 new lipophilic monocationic gallium(III) complexes prepared from $N_4O_2^{2-}$ Schiff base ligands (Figure 1 and Table 1) containing alkoxy, alkyl, and/or alkylamino substituents on the aromatic rings of the ligand.

Results and Discussion

Cold Chemistry. The 10 new ^{67}Ga-labeled gallium(III) bis(salicylaldimine) complexes (Table 1) were synthesized using previously described methods.[11] The tris(salicylaldimine) ligand precursors were prepared

* Address for correspondence: Mark A. Green, Purdue University, 1333 Pharmacy Building, West Lafayette, IN 47907-1333. Tel: (317) 494-1441. Fax: (317) 494-6790.

® Abstract published in *Advance ACS Abstracts*, November 1, 1994.

0022-2623/94/1837-4400$04.50/0

Table 1. Gallium(III) Bis(salicylaldimine) Complexes Studied

compd	ligand	R	R_4	R_5	R_6	$^{67}GaL^+$ log P^a
1	$(sal)_2$BAPEN	H	H	H	H	0.84 ± 0.02
2	$(5\text{-MeOsal})_2$BAPEN	H	H	OCH_3	H	0.75 ± 0.01
3	$(4\text{-MeOsal})_2$BAPEN	H	OCH_3	H	H	1.10 ± 0.03
4	$(4\text{-MeO-6-Mesal})_2$BAPEN	H	OCH_3	H	CH_3	1.60 ± 0.03
5	$(4,6\text{-}(MeO)_2sal)_2$BAPEN	H	OCH_3	H	OCH_3	1.96 ± 0.05[b]
6	$(4\text{-MeO-5-Mesal})_2$BAPEN	H	OCH_3	CH_3	H	2.12 ± 0.06[b]
7	$(4\text{-EtO-6-Mesal})_2$BAPEN	H	OCH_2CH_3	H	CH_3	2.01 ± 0.07
8	$(5\text{-}i\text{-Prsal})_2$BAPEN	H	H	*i*-Pr	H	2.96 ± 0.04
9	$(4\text{-deasal})_2$BAPEN	H	NEt_2	H	H	2.59 ± 0.13[b]
10	$(4,6\text{-}(MeO)_2sal)_2Me_4$BAPEN	CH_3	OCH_3	H	OCH_3	2.88 ± 0.05
11	$(4\text{-deasal})_2Me_4$BAPEN	CH_3	NEt_2	H	H	3.00 ± 0.07

[a] *P* is the octanol/water partition coefficient determined for the ^{67}Ga-labeled complex ($n = 4$). [b] $n = 6$.

Scheme 1

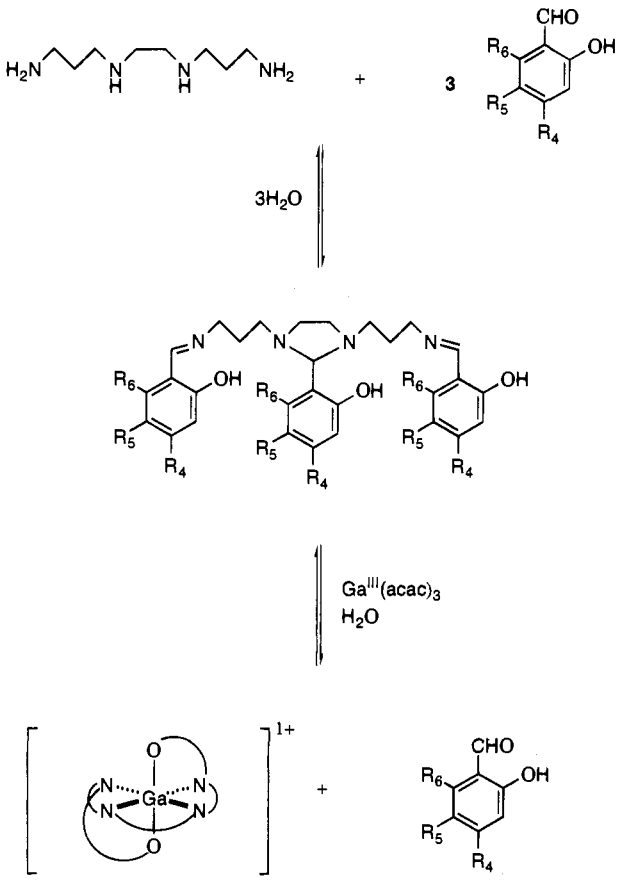

and isolated by condensation of the appropriate linear tetraamine (either bis(3-aminopropyl)ethylenediamine, BAPEN, or bis(2,2-dimethyl-3-aminopropyl)ethylenediamine, DM-BAPEN) with the corresponding salicylaldehyde derivative (Scheme 1). Reactions of these tris(salicylaldimines) with tris(acetylacetonato)gallium(III), $Ga(acac)_3$, in ethanol results in hydrolytic cleavage of the bridging imino group and formation of the desired cationic gallium(III) bis(salicylaldimine) complexes (Scheme 1). The general structure of the bis(salicylaldimine) ligand is shown in Figure 1. Similar chemistry has been reported in the literature where the tris(salicylaldimine) of triethylenetetraamine reacts with metal ions, including gallium(III), in aqueous solution to give the corresponding bis(salicylaldimino) complexes.[12,13] Proton NMR and mass spectra of the 10 new complexes prepared with stable Ga confirm loss of the bridging imino group.

X-ray crystallographic characterization of one of these complexes, Ga[bis[(4,6-dimethoxysalicyl)aldimino]-*N*,*N*'-bis(2,2-dimethyl-3-aminopropyl)ethylenediamine]$^+$ I^- (**10**),

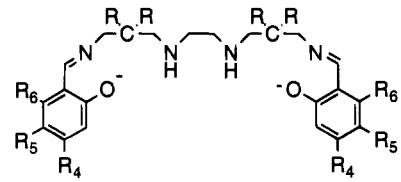

Figure 1. General structural formula for the hexadentate bis(salicylaldimine) ligands.

shows that all six potential donor atoms of the ligand coordinate to provide a complex with a distorted octahedral $N_4O_2^{2-}$ geometry around the gallium(III) center (Figure 2 and Table 2). The gallium(III) center is coordinated by two amine and two imine nitrogen lone pairs and two deprotonated phenolic oxygens, resulting in a complex with an overall +1 charge. The Ga—O bond distances (1.937 and 1.932 Å) and Ga—N bond distances (2.011, 2.101, 2.084, and 2.039 Å) are within the range of values reported for six-coordinate gallium Schiff base complexes previously described.[4,5,14] The phenolic oxygens in this complex are shown to be coordinated in a *trans* configuration, contrasting with the *cis* arrangement found in the iron(III) complex of the similar bis(salicylaldimino)triethylenetetraamine ligand.[15]

Radiochemistry and Animal Studies. The no-carrier-added ^{67}Ga complexes of the bis(salicylaldimine) ligands were prepared analogous to the method of cold complex formation in which $Ga(acac)_3$ is reacted with the tris(salicylaldimine) ligand precursor in ethanol. The radiochemical purity of the radiotracers was always found to exceed 98% by thin layer chromatography. Although these complexes are cationic, they are also lipophilic (Table 1) with log *P* values ranging from 0.8 to 3.0 (where *P* is the measured octanol/water partition coefficient). As expected, the lipophilicity of these compounds increases with increasing alkyl substitution of either the tetraamine backbone or the aromatic rings. Complex lipophilicity was found to depend somewhat on the position of the alkyl or alkoxy group on the aromatic rings. For example, a methoxy group in position 5 of the two aromatic rings has virtually no effect on log *P*, while 4-methoxy substitution of both rings increases log *P* by 0.26 (compare compounds **1**—**3**). Similarly, a methyl group in position 5 of the two aromatic rings increases log *P* by 0.50, while 6-methyl substitution of these rings increases log *P* by 1.02 (compare the log *P* values for compounds **3**, **4**, and **6**, Table 1).

The biodistribution of each ^{67}Ga bis(salicylaldimine) complex was determined in Sprague—Dawley rats at time points ranging from 1 min to 2 h following femoral vein injection of the radiotracer. To insure that the

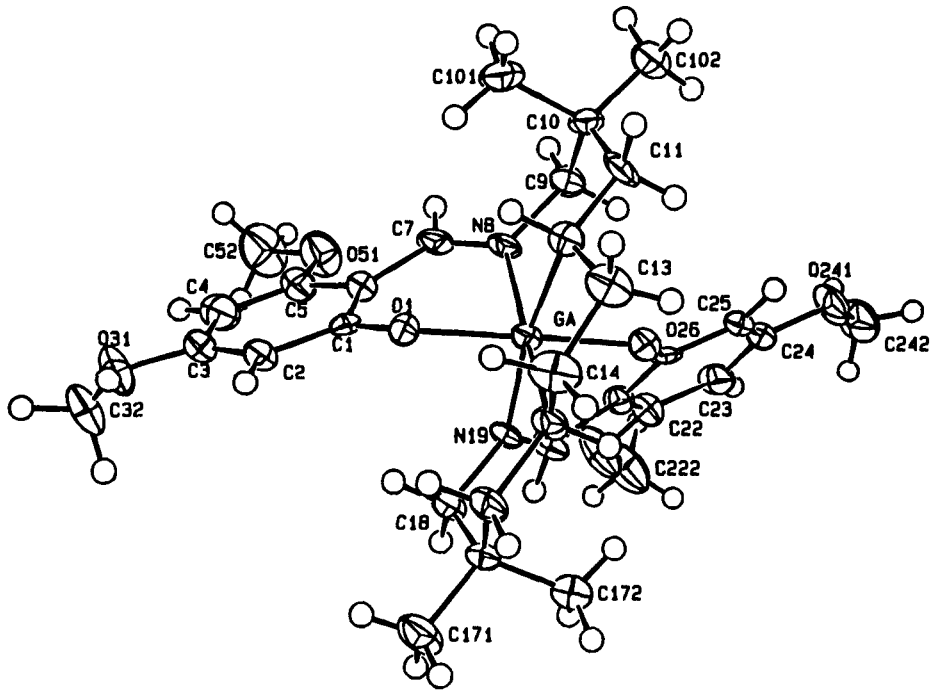

Figure 2. ORTEP drawing of the molecular structure of Ga[(4,6-(MeO)$_2$sal)$_2$Me$_4$BAPEN]$^+$ illustrating the *trans* configuration of the phenolic oxygens around Ga^{3+}. Selected bond distances and angles are given in Table 2.

Table 2. Selected Bond Lengths (Å) and Angles (deg) for Compound **10**

	Bond Lengths		
Ga–O1	1.937(6)	Ga–N19	2.039(8)
Ga–O26	1.932(6)	N8–C7	1.29(1)
Ga–N8	2.011(8)	N19–C20	1.28(1)
Ga–N12	2.101(8)	C1–O1	1.32(1)
Ga–N15	2.084(8)	C26–O26	1.32(1)
	Bond Angles		
O1–Ga–O26	179.4(3)	O26–Ga–N19	87.4(3)
O1–Ga–N8	87.6(3)	N8–Ga–N12	89.5(3)
O1–Ga–N12	92.7(3)	N8–Ga–N15	172.3(3)
O1–Ga–N15	89.5(3)	N8–Ga–N19	98.3(3)
O1–Ga–N19	92.7(3)	N12–Ga–N15	83.5(3)
O26–Ga–N8	93.0(3)	N12–Ga–N19	170.6(3)
O26–Ga–N12	87.1(3)	N15–Ga–N19	88.9(3)
O26–Ga–N15	89.9(3)		

Table 3. Myocardial Levels of Tracer Gallium after Intravenous Administration of Gallium-67 Bis(salicylaldimine) Complexes to Rats

		percent of injected dose in heart	
	ligand	1 min	120 min
1	(sal)$_2$BAPEN	0.45 ± 0.01	0.41 ± 0.03
2	(5-MeOsal)$_2$BAPEN	0.34 ± 0.03	0.23 ± 0.03
3	(4-MeOsal)$_2$BAPEN	0.67 ± 0.08	0.65 ± 0.05
4	(4-MeO-6-Mesal)$_2$BAPEN	1.08 ± 0.09	1.03 ± 0.05
5	(4,6-(MeO)$_2$sal)$_2$BAPEN	1.04 ± 0.12	0.86 ± 0.11
6	(4-MeO-5-Mesal)$_2$BAPEN	0.88 ± 0.06	0.89 ± 0.03
7	(4-EtO-6-Mesal)$_2$BAPEN	0.91 ± 0.04	0.87 ± 0.02
8	(5-*i*-Prsal)$_2$BAPEN	0.67 ± 0.08	0.55 ± 0.04
9	(4-deasal)$_2$BAPEN	0.69 ± 0.05	0.65 ± 0.05
10	(4,6-(MeO)$_2$sal)$_2$Me$_4$BAPEN	1.03 ± 0.17	1.01 ± 0.06
11	(4-deasal)$_2$Me$_4$BAPEN	0.66 ± 0.06	0.40 ± 0.04

complexes and excess ligand present in the aqueous solution remained solubilized, propylene glycol was added as 5–10% of the total volume for the most lipophilic derivatives.[16] The biodistribution data for these compounds are reported as percentage of the injected dosage per organ in Tables 3–7. All of the complexes show myocardial uptake (ranging from 0.3 to 1% of the injected dose) and myocardial retention of

Table 4. Liver Levels of Tracer Gallium after Intravenous Administration of Gallium-67 Bis(salicylaldimine) Complexes to Rats

		percent of injected dose in liver	
	ligand	1 min	120 min
1	(sal)$_2$BAPEN	26.7 ± 3.2	5.3 ± 0.6
2	(5-MeOsal)$_2$BAPEN	26.5 ± 4.7	6.8 ± 0.4
3	(4-MeOsal)$_2$BAPEN	25.2 ± 1.3	5.1 ± 1.4
4	(4-MeO-6-Mesal)$_2$BAPEN	28.8 ± 2.0	3.4 ± 0.5
5	(4,6-(MeO)$_2$sal)$_2$BAPEN	43.0 ± 3.6	3.1 ± 0.2
6	(4-MeO-5-Mesal)$_2$BAPEN	39.5 ± 2.2	5.3 ± 0.3
7	(4-EtO-6-Mesal)$_2$BAPEN	29.5 ± 2.6	3.0 ± 0.3
8	(5-*i*-Prsal)$_2$BAPEN	49.2 ± 0.8	8.5 ± 1.0
9	(4-deasal)$_2$BAPEN	38.1 ± 3.0	9.7 ± 1.6
10	(4,6-(MeO)$_2$sal)$_2$Me$_4$BAPEN	50.6 ± 5.7	3.9 ± 0.2
11	(4-deasal)$_2$Me$_4$BAPEN	47.0 ± 6.5	11.1 ± 2.5

the radiolabel over the 2 h of the study (Table 3). Thus, it seems that myocardial retention of tracer is observed as a general characteristic of monocationic gallium complexes of this type.

Myocardial uptake was found to increase with lipophilicity up to a log *P* value of ~1. For compounds with log *P* values greater than 1, myocardial uptake appears sensitive to the presence of an alkoxy group on the ring. Compounds **4**–**7** and **10** have alkoxy groups in position 4 on the ring, as well as other groups to insure that the compound maintains a log *P* value above 1. These five derivatives all provide the same myocardial uptake of tracer at ~1% of the injected dose, despite a wide log *P* range from 1.6 to 2.9. By contrast, the similarly lipophilic compounds lacking an alkoxy group on the ring, but having either an alkyl group in position 5 or an alkylamino group in position 4 (compounds **8**, **9**, and **11**), have a lower heart uptake at ~0.7% of the injected dose.

In addition to high myocardial uptake, to be useful in imaging the heart a radiotracer must also clear rapidly from tissues surrounding the heart. All of these radiotracers exhibit relatively low uptake in the lungs and are observed to clear relatively rapidly from blood,

Table 5. Blood Levels of Tracer Gallium after Intravenous Administration of Gallium-67 Bis(salicylaldimine) Complexes to Rats

	ligand	percent of injected dose in blood 1 min	120 min
1	$(sal)_2$BAPEN	4.21 ± 0.06	0.64 ± 0.10
2	$(5\text{-MeOsal})_2$BAPEN	7.55 ± 1.45	1.11 ± 0.04
3	$(4\text{-MeOsal})_2$BAPEN	4.44 ± 0.33	0.42 ± 0.03
4	$(4\text{-MeO-6-Mesal})_2$BAPEN	5.94 ± 1.23	0.43 ± 0.04
5	$(4,6\text{-(MeO)}_2\text{sal})_2$BAPEN	8.49 ± 1.41	0.33 ± 0.02
6	$(4\text{-MeO-5-Mesal})_2$BAPEN	7.79 ± 0.09	0.61 ± 0.01
7	$(4\text{-EtO-6-Mesal})_2$BAPEN	7.73 ± 1.05	0.42 ± 0.03
8	$(5\text{-}i\text{-Prsal})_2$BAPEN	23.4 ± 0.9	1.21 ± 0.04
9	$(4\text{-deasal})_2$BAPEN	11.1 ± 0.30	1.27 ± 0.14
10	$(4,6\text{-(MeO)}_2\text{sal})_2\text{Me}_4$BAPEN	18.8 ± 6.9	0.45 ± 0.03
11	$(4\text{-deasal})_2\text{Me}_4$BAPEN	30.6 ± 3.5	1.06 ± 0.20

Table 6. Lung Levels of Tracer Gallium after Intravenous Administration of Gallium-67 Bis(salicylaldimine) Complexes to Rats

	ligand	percent of injected dose in lungs 1 min	120 min
1	$(sal)_2$BAPEN	1.00 ± 0.09	0.28 ± 0.04
2	$(5\text{-MeOsal})_2$BAPEN	0.79 ± 0.16	0.18 ± 0.01
3	$(4\text{-MeOsal})_2$BAPEN	1.05 ± 0.13	0.38 ± 0.03
4	$(4\text{-MeO-6-Mesal})_2$BAPEN	0.88 ± 0.13	0.55 ± 0.03
5	$(4,6\text{-(MeO)}_2\text{sal})_2$BAPEN	0.92 ± 0.21	0.52 ± 0.08
6	$(4\text{-MeO-5-Mesal})_2$BAPEN	0.79 ± 0.01	0.42 ± 0.04
7	$(4\text{-EtO-6-Mesal})_2$BAPEN	0.80 ± 0.12	0.49 ± 0.01
8	$(5\text{-}i\text{-Prsal})_2$BAPEN	1.06 ± 0.04	0.36 ± 0.05
9	$(4\text{-deasal})_2$BAPEN	1.26 ± 0.14	0.67 ± 0.04
10	$(4,6\text{-(MeO)}_2\text{sal})_2\text{Me}_4$BAPEN	1.63 ± 0.47	0.64 ± 0.06
11	$(4\text{-deasal})_2\text{Me}_4$BAPEN	5.30 ± 0.23	1.31 ± 0.07

Table 7. Kidney Levels of Tracer Gallium after Intravenous Administration of Gallium-67 Bis(salicylaldimine) Complexes to Rats

	ligand	percent of injected dose in each kidney 1 min	120 min
1	$(sal)_2$BAPEN	9.84 ± 0.65	1.40 ± 0.25
2	$(5\text{-MeOsal})_2$BAPEN	7.64 ± 0.16	1.19 ± 0.05
3	$(4\text{-MeOsal})_2$BAPEN	8.42 ± 0.81	1.69 ± 0.08
4	$(4\text{-MeO-6-Mesal})_2$BAPEN	5.39 ± 0.25	1.94 ± 0.18
5	$(4,6\text{-(MeO)}_2\text{sal})_2$BAPEN	5.26 ± 0.69	2.17 ± 0.17
6	$(4\text{-MeO-5-Mesal})_2$BAPEN	5.14 ± 0.37	2.74 ± 0.21
7	$(4\text{-EtO-6-Mesal})_2$BAPEN	5.24 ± 0.31	2.42 ± 0.17
8	$(5\text{-}i\text{-Prsal})_2$BAPEN	6.02 ± 0.35	3.95 ± 0.14
9	$(4\text{-deasal})_2$BAPEN	6.33 ± 0.20	4.67 ± 0.19
10	$(4,6\text{-(MeO)}_2\text{sal})_2\text{Me}_4$BAPEN	8.33 ± 0.80	5.40 ± 0.24
11	$(4\text{-deasal})_2\text{Me}_4$BAPEN	4.25 ± 0.52	5.17 ± 0.19

liver, and kidneys (Tables 4–7). While the initial liver uptake of these compounds is very high due to their lipophilicity, by 2 h postinjection heart-to-liver ratios generally exceed 1 due to further tracer clearance into the bile (Table 8). Since all of these compounds are retained in myocardium but are cleared from the liver, the heart-to-liver ratios always increase with time postinjection. The best results were again consistently obtained with tracers containing alkoxy substituents (Table 8).

Fast tracer clearance from the blood was observed for all of these compounds. As with clearance from the liver, an alkyl or alkoxy substituent at the 5 position or an alkylamino substitutent at the 4 position of the aromatic rings significantly reduces the rate of clearance from the blood (Tables 5 and 9). Unfortunately, none of these new tracers provide better heart-to-blood ratios (Table 9) than the lead compound (**5**, Table 1).

Conclusion

The biodistribution data for this series of compounds suggest that myocardial uptake and retention are general characteristics for this class of gallium radiopharmaceuticals. While the modifications made to the ligand structure resulted in compounds that match the favorable characteristics of lead compound **5** in rat biodistribution studies, none of the modifications resulted in an improvement on the biological properties of that lead compound. Further studies remain underway to synthesize and evaluate related Ga complexes functionalized at other sites in the ligand backbone and containing a more diverse selection of peripheral substituents.

Experimental Section

Salicylaldehyde, triethylenetetraamine·xH_2O, 4-methoxysalicylaldehyde, 4,6-dimethoxysalicylaldehyde, 5-methoxysalicylaldehyde, *N,N'*-bis(3-aminopropyl)ethylenediamine, and 4-(diethylamino)salicylaldehyde were obtained from Aldrich Chemical Co. Gallium(III) acetylacetonate was purchased from Strem Chemicals, Inc. *N,N'*-Bis(2,2-dimethyl-3-aminopropyl)ethylenediamine was synthesized by haloalkylation of 2,2-dimethylpropanediamine with 1,2-dibromoethane using a general literature method for synthesis of linear tetraamines.[19] New aldehydes were synthesized by formylation of the substituted phenol or alkylation of hydroxyl groups on the aromatic ring: 5-isopropylsalicylaldehyde was synthesized by formylation of 4-isopropylphenol as reported in the literature.[20] 4-Methoxy-6-methylsalicylaldehyde and 4-methoxy-5-methylsalicylaldehyde were synthesized as described in the literature;[21] 4-ethoxy-6-methylsalicylaldehyde was synthesized similarly, using diethyl sulfate. Gallium-67 chloride in 0.1 N HCl solution was obtained from Nordion International, Inc., Kanata, Ontario, and Mallinckrodt Medical, Inc., St. Louis, MO. Gallium-68 chloride was obtained in 1 N HCl from an ionic $^{68}Ge/^{68}Ga$ SnO_2-based generator[2] purchased from DuPont/New England Nuclear, N. Billerica, MA.

Proton NMR spectra were obtained on a Varian VXR-500S spectrometer in $CDCl_3$ or Me_2SO-d_6 containing tetramethylsilane as reference. FTIR spectra were obtained on a Perkin Elmer FTIR spectrometer in KBr pellets. Melting points were determined in open capillary tubes using a Gallenkamp melting point apparatus. Radiochromatograms were analyzed with a Berthold Tracemaster 20 automatic TLC linear analyzer. All animal studies were carried out in accordance with procedures approved by the Purdue Animal Care and Use Committee.

The tris(salicylaldimine) ligand precursors were synthesized by condensation of 3 equiv of the appropriate salicylaldehyde with one of the tetraamines in ethanol. The corresponding cationic gallium(III) bis(salicylaldimine) complexes were synthesized by one of two methods: the ligand exchange reaction between $Ga(acac)_3$ and the tris(salicylaldimine) ligand precursor as described in the literature,[5a] in which the bridging imino is hydrolyzed upon coordination to the gallium; or an in-situ reaction in which 2 equiv of the aldehyde are condensed with an equivalent of the appropriate tetraamine.[12,13] The free bis(salicylaldimine) ligands were never isolated. A more detailed description of the synthesis of one tris(salicylaldimine) and its gallium bis(salicylaldimine) complex is given below.

Synthesis of H_3[$(4,6\text{-MeO}_2\text{sal})_3$DM-BAPEN]. To a solution of 1.00 g of 4,6-dimethoxysalicylaldehyde (5.49 mmol) in 15 mL of dry methanol was added 0.42 g of *N,N'*-bis(2,2-dimethyl-3-aminopropyl)ethylenediamine (1.84 mmol) in 15 mL of dry methanol. The mixture was refluxed for 20 min and then allowed to stir until cooled to 25 °C. The solvent was removed by rotary evaporation and the resulting yellow oil dissolved in diethyl ether. Unreacted aldehyde immediately precipitated and was removed by filtration. The filtrate was cooled to 0 °C for approximately 24 h, and the bright yellow product that precipitated was filtered and washed with cold diethyl ether; 40% yield. ^{1}H-NMR at 500 MHz in deuterated chloroform with TMS as reference: δ 0.82 (s, 6H), 0.85 (s, 6H,

Table 8. Heart-to-Liver Ratios of Tracer Gallium after Intravenous Administration of Gallium-67 Bis(salicylaldimine) Complexes to Rats

		heart-to-liver ratios[a]		
		1 min	15 min	120 min
1	$(sal)_2$BAPEN	0.20 ± 0.02	0.51 ± 0.06	0.9 ± 0.2
2	$(5\text{-MeOsal})_2$BAPEN	0.15 ± 0.03	0.19 ± 0.05	0.42 ± 0.03
3	$(4\text{-MeOsal})_2$BAPEN	0.32 ± 0.05	0.62 ± 0.15	1.6 ± 0.7
4	$(4\text{-MeO-6-Mesal})_2$BAPEN	0.45 ± 0.08	–	3.6 ± 0.6
5	$(4,6\text{-}(MeO)_2sal)_2$BAPEN	0.32 ± 0.03	0.56 ± 0.10	4.1 ± 0.4
6	$(4\text{-MeO-5-Mesal})_2$BAPEN	0.14 ± 0.01	–	1.92 ± 0.13
7	$(4\text{-EtO-6-Mesal})_2$BAPEN	0.29 ± 0.02	0.73 ± 0.03	2.7 ± 0.2
8	$(5\text{-}i\text{-Prsal})_2$BAPEN	0.16 ± 0.02	–	0.75 ± 0.03
9	$(4\text{-deasal})_2$BAPEN	0.24 ± 0.03	0.28 ± 0.04	0.86 ± 0.18
10	$(4,6\text{-}(MeO)_2sal)_2$DM-BAPEN	0.23 ± 0.06	0.32 ± 0.02	3.24 ± 0.07
11	$(4\text{-deasal})_2$DM-BAPEN	0.17 ± 0.03	0.13 ± 0.04	0.50 ± 0.07

[a] Calculated from the percent of injected dose per gram of tissue values.

Table 9. Heart-to-Blood Ratios of Tracer Gallium after Intravenous Administration of Gallium-67 Bis(salicylaldimine) Complexes to Rats

		heart-to-blood ratios[a]		
		1 min	15 min	120 min
1	$(sal)_2$BAPEN	2.15 ± 0.05	8.3 ± 0.7	12.2 ± 0.4
2	$(5\text{-MeOsal})_2$BAPEN	0.89 ± 0.12	2.6 ± 0.6	4.3 ± 0.3
3	$(4\text{-MeOsal})_2$BAPEN	2.99 ± 0.15	17.6 ± 0.3	30.6 ± 2.2
4	$(4\text{-MeO-6-Mesal})_2$BAPEN	3.4 ± 0.6	–	45.1 ± 3.3
5	$(4,6\text{-}(MeO)_2sal)_2$BAPEN	2.3 ± 0.4	18.1 ± 0.9	45.6 ± 4.0
6	$(4\text{-MeO-5-Mesal})_2$BAPEN	2.1 ± 0.2	–	30.0 ± 1.3
7	$(4\text{-EtO-6-Mesal})_2$BAPEN	2.2 ± 0.2	20.9 ± 0.6	40.5 ± 1.5
8	$(5\text{-}i\text{-Prsal})_2$BAPEN	0.54 ± 0.07	–	8.6 ± 0.6
9	$(4\text{-deasal})_2$BAPEN	1.22 ± 0.08	4.5 ± 0.3	9.2 ± 1.1
10	$(4,6\text{-}(MeO)_2sal)_2$DM-BAPEN	1.1 ± 0.4	9.6 ± 0.5	44.5 ± 1.6
11	$(4\text{-deasal})_2$DM-BAPEN	0.45 ± 0.04	1.9 ± 0.3	8.1 ± 1.6

[a] Calculated from the percent of injected dose per gram of tissue values.

CH_3), 2.25 (m, 2H), 2.52 (m, 6H), 2.65 (m, 2H), 2.92 (m, 2H), 3.30 (m, 6H, CH_2C), 3.71 (m, 6H), 3.76 (s, 12H, OCH_3), 4.43 (s, 1H, NCHN), 5.72 (m, 6H, C_6H_2), 8.14 (m, 2H, CH=N). IR (KBr disk): ν(C=N) 1624 cm^{-1}. The fast-atom bombardment mass spectrum in positive ion mode (DTT/DTE matrix) showed $[M + H]^+$ at m/z = 721 for M = $C_{39}H_{52}N_4O_9$.

Tris(salicylaldimine)BAPEN,[22a] tris[(5-methoxysalicyl)aldimine]BAPEN,[22b] tris[(4-methoxysalicyl)aldimine]BAPEN,[22c] tris[(4-methoxy-6-methylsalicyl)aldimine]BAPEN,[22d] tris[(4,6-dimethoxysalicyl)aldimine]BAPEN,[11] tris[(4-methoxy-5-methylsalicyl)aldimine]BAPEN,[22e] tris[(4-ethoxy-6-methylsalicyl)-aldimine]BAPEN,[22f] tris[(5-isopropylsalicyl)aldimine]BAPEN,[22g] tris[[4-(diethylamino)salicyl]aldimine]BAPEN,[22h] and tris[[4-(diethylamino)salicyl]aldimine]DM-BAPEN[22i] were synthesized similarly.

Synthesis of Ga[(4,6-(MeO)$_2$sal)$_2$DM-BAPEN]$^+$I$^-$. A solution of 110 mg of $Ga(acac)_3$ (0.3 mmol) in 10 mL of warm ethanol was added to 216 mg of H_3[(4,6-MeO_2sal)$_3$DM-BAPEN] (0.3 mmol) in 10 mL of warm ethanol. The mixture was heated to reflux for 30 min, and 50 mg of KI in 1 mL of water was then added to the hot ethanol solution. The solution was slowly cooled to room temperature. The product precipitated out of solution as a white microcrystalline solid upon cooling; 86% yield, decomposes without melting at 298 °C. ^{1}H-NMR at 500 MHz in dimethylsulfoxide-d_6 with TMS as reference: δ 0.77, 0.91 (s, 12H, CCH_3), 2.75 (m, 4H), 3.27 (m, 4H), 3.68 (m, 4H, CH_2), 3.75 (s, 6H), 3.78 (s, 6H, OCH_3), 4.70 (br s, 2H, NH), 5.90 (m, 4H, C_6H_2), 8.10 (m, 2H, CH=N). IR (KBr disk): ν(C=N) 1603 cm^{-1}. The positive ion fast-atom bombardment mass spectrum (DTT/DTE matrix) showed $[M]^+$ at m/z = 625 for $[C_{30}H_{44}N_4O_6Ga]^+$.

[Gallium(III) bis(salicylaldimino)BAPEN]$^+$I$^-$,[23a] [gallium(III) bis[(5-methoxysalicyl)aldimino)BAPEN]$^+$I$^-$,[23b] [gallium(III) bis[(4-methoxysalicyl)aldimino]BAPEN]$^+$I$^-$,[23c] [gallium(III) bis[(4-methoxy-6-methylsalicyl)aldimino]BAPEN]$^+$I$^-$,[23d] [gallium(III) bis[(4,6-dimethoxysalicyl)aldimino]BAPEN]$^+$I$^-$,[11] [gallium(III) bis[(4-methoxy-5-methylsalicyl)aldimino]-BAPEN]$^+$I$^-$,[23e] [gallium(III) bis[(4-ethoxy-6-methylsalicyl)-aldimino]BAPEN]$^+$I$^-$,[23f] [gallium(III) bis[(5-isopropylsalicyl)-aldimino]BAPEN]$^+$I$^-$,[23g] [gallium(III) bis[[4-(diethylamino)-salicyl]aldimino]BAPEN]$^+$I$^-$,[23h] and [gallium(III) bis[[4-(diethylamino)salicyl]aldimino]DM-BAPEN]$^+$I$^-$[23i] were prepared similarly.

X-ray Crystallography. Crystals of Ga[(4,6-(MeO_2)sal)$_2$-DM-BAPEN]$^+$I$^-$×e1·H_2O were grown by evaporation of CH_3-CN from a solution of the complex in 1:1 CH_3CN/H_2O. The complex crystallizes in the monoclinic $P2_1/n$ (no. 14) space group established by the systematic absences: $h0l$ $h + 1 = 2n$, $0k0$ $k = 2n$. The monoclinic cell parameters are a = 8.515(2) Å, b = 24.243(4) Å, c = 16.382(3) Å, β = 102.34(1)°, V = 3303.7(2) Å^3, Z = 4. fw is 771.35 for $C_{30}H_{46}N_4O_7GaI$, and the calculated density is 1.55 g/cm^3. A colorless plate of approximate dimensions 0.45 × 0.39 × 0.25 mm^3 was mounted on a glass fiber in a random orientation. Preliminary examination and data collection were both performed on an Enraf Nonius CAD4 diffractometer equipped with a graphite crystal, incident beam monochromator with Mo K_α radiation (λ = 0.71073 Å) at 293 K. The cell constants and an orientation matrix for data collection were obtained from least-squares refinement using the setting angles of 25 reflections in the range 17° < ϑ < 20°.

Data was collected at 298 K using variable speed $\omega - 2\vartheta$ scans with the scan rate varying from 2° to 16° per minute. 2ϑ max = 45°. A total of 4425 reflections were collected, of which 4425 were unique. Lorentz and polarization corrections were applied. An empirical absorption correction was also applied.[24] Relative transmission coefficients ranged from 0.580 to 1.000 with an average value of 0.747.

The structure was solved using SHELX-86.[25] The atoms were located in succeeding difference Fourier syntheses. Locations of hydrogen atoms were added to the structure factor but not refined. The overall structure was refined in full-matrix least-squares where the function minimized was $\Sigma(|F_o| - |F_c|)^2$ and the weight w is defined by the Killean and Lawrence method with terms of 0.020 and 1.0.[26] Scattering factors were taken from ref 27. Anomalous dispersion effects[28] were included in F_c, and the values for f' and f'' were also taken from ref 27. The 3167 reflections having intensities greater than 3 times their standard deviations were used in refinements. The final refinement cycle included 383 variable parameters and converged with unweighted and weighted

agreement factors of $R_1 = \Sigma|F_o - F_c|/\Sigma F_o = 0.069$ and $R_2 = \mathrm{SQRT}(\Sigma\omega(F_o - F_c)^2/\Sigma\omega F_o^2) = 0.087$, respectively. Refinement was done using MolEN. The highest peak in the final difference Fourier map had a height of 1.26 e/A^3 with an estimated eror based on ∂F of 0.17. No unusual trends were seen. Important bond lengths and angles are listed in Table 2.

Synthesis and Characterization of Radiolabeled Complexes. Gallium-67 chloride in HCl solution was evaporated by heating under a stream of N_2 in a borosilicate test tube. While still under N_2, the residue was redissolved in 50–100 μL of an ethanol solution containing 0.002% by weight acetylacetone. The no-carrier-added [^{67}Ga]gallium(III) tris(acetylacetonate) solution was then transferred to a clean test tube, and 0.5–1.0 mg of the tris(salicylaldimine) ligand (5–10 mg/mL of ethanol) was added. The ethanol solution was mixed and then heated for 10–20 min in a 65 °C water bath to assure reaction completion. The reaction solution was then diluted to 5% ethanol with a saline solution (0.16 M NaCl) and from 5 to 10% propylene glycol, depending on the lipophilicity of the complex. The diluted solutions were filtered through a sterile 0.2 μm sterile poly(tetrafluoroethylene) filter (Millipore Corp., Bedford, MA) to deliver a product suitable for intravenous injection. The ^{68}Ga-labeled complexes were similarly prepared.

The radiochemical purity of the ^{67}GaL$^+$ and ^{68}GaL$^+$ complexes were always found to exceed 98% using thin layer chromatography on C_{18} reversed phase plates eluted with either methanol or methanol containing 10% by volume saline (0.16 M NaCl). R_f values ranged from 0.05 to 0.2 with methanol eluant and from 0.4 to 0.7 with 90% methanol/10% saline eluant. The uncomplexed Ga^{3+} ion and unreacted Ga(acac)$_3$ remained at the origin (R_f =0.0) under both chromatographic conditions. Specifically, using 90% methanol/10% saline eluant, R_f values of 0.72, 0.69, 0.71, 0.65, 0.61, 0.59, 0.56, 0.52, 0.51, 0.53, and 0.45 were obtained for the ^{67}Ga/^{68}Ga compounds of ligands **1**–11, respectively.

Partition coefficients of the $^{67/68}$GaL$^+$ radiotracers were measured following 1 min of vigorous vortex mixing of 1 mL of 1-octanol and 1 mL of isotonic Tris-buffered saline (pH = 7)[29] with approximately 0.1 μCi of the radiolabeled gallium complex. Following centrifugation at >1200*g* for 5 min, the octanol and aqueous phases were sampled and counted in an automatic well counter; 500 μL of the octanol phase from this partitioning was repartitioned two to three times with fresh buffer to insure that trace hydrophilic ^{67}Ga impurities did not alter the calculated *P* values. The reported log *P* values are the average of the second and third (or third and fourth) extractions from two to three independent measurements, so that the log *P* values in Table 1 represent the mean (± standard deviation) of four to six measurements.

Rat Biodistribution Studies. The no-carrier-added ^{67}Ga bis(salicylaldimine) complex (1–3 μCi, 0.1–0.2 mL) was administered by bolus injection with a 27 gauge needle into the femoral vein of male Sprague-Dawley rats under surgical anesthesia with diethyl ether. The dose administered to each animal was quantitated by weighing the injection syringe on an analytical balance before and after injection. The ether-anesthetized rats were sacrificed by decapitation at 1, 15, or 120 min postinjection. The organs of interest were excised, blotted to remove surface blood, and weighed, and the tissue radioactivity was measured in an automatic γ counter. A standard, composed of a measured aliquot of a known mass of the injectate, was counted along with the tissue samples for quantitation of the injected dose for each animal. Radiopharmaceutical biodistribution was then calculated as a percentage of the injected dose per gram of tissue and as a percentage of the injected dose per organ for each tissue sample. Blood was assumed to account for 7% of total body mass. The biodistribution data reported in Tables 3–9 represent the mean (± standard deviation) of three to four measurements.

Acknowledgment. Support for this research was provided by a postdoctoral fellowship to B.W.T. from the American Heart Association, Indiana Affiliate, and a grant from the National Cancer Institute (RO1-CA46909).

Supplementary Material Available: Tables of positional parameters, bond lengths, bond angles, and anisotropic displacement coefficients for compound **10**; complete tables of biodistribution data for each ^{67}Ga compound in rats calculated as the percentage of the injected dose per gram of tissue; and rat biodistribution data for [^{67}Cu]PTSM in the presence and absence of propylene glycol excipient (25 pages). Ordering information is given on any current masthead page.

References

(1) (a) Ter-Pogossian, M. M.; Raichle, M. E.; Sobel, B. E. Positron-Emission Tomography. *Sci. Am.* **1980**, *243*, 170–181. (b) Reivich, M., Alavi, A., Eds. *Positron Emission Tomography*; A. R. Liss: New York, 1985. (c) Phelps, M. E., Mazziotta, J. C., Schelbert, H. R., Eds. *Positron Emission Tomography and Autoradiography Principles and Applications for the Brain and Heart.* Raven Press: New York, 1986. (d) Fowler, J. S.; Hoffman, E. J.; Larson, S. M.; Scheibert, H. R.; Schwaiger, M.; Wagner, H. N.; Wolf, A. P.; Hendee, W. R. Cyclotrons and Radiopharmaceuticals in Positron Emission Tomography. *J. Am. Med. Assoc.* **1988**, *259* (12), 1854–1860. (e) Green, M. A. Metal Radionuclides in Diagnostic Imaging by Positron Emission Tomography. In *Advances in Metals in Medicine*; Abrams, M. J., Murrer, B. A., Eds.; JAI Press Inc.: Greenwich, CT, 1993 Vol. 1, pp 75–114.

(2) Loc'h, C.; Maziere, B.; Comar, D. A New Generator for Ionic Gallium-68. *J. Nucl. Med.* **1980**, *21*, 171–173.

(3) Green, M. A. The Potential for Generator-Based PET Perfusion Tracers. *J. Nucl. Med.* **1990**, *31*, 1641–1645.

(4) (a) Green, M. A. Gallium and Copper Radiopharmaceutical Chemistry. In *New Trends in Radiopharmaceutical Synthesis, Quality Assurance, and Regulatory Control*; Emran, A. M., Ed.; Plenum Press: New York, 1991; p 119. (b) Green, M. A.; Welch, M. J. Gallium Radiopharmaceutical Chemistry. *Nucl. Med. Biol.* **1989**, *16*, 435–448.

(5) (a) Green, M. A.; Welch, M. J.; Mathias, C. J.; Fox, K. A. A.; Knabb, R. M.; Huffman, J. C. Gallium-68 1,1,1-tris(5-methoxysalicylaldiminomethyl)ethane: A Potential Tracer for Evaluation of Regional Myocardial Blood Flow. *J. Nucl. Med.* **1985**, *26*, 170–180. (b) Green, M. A.; Mathias, C. J.; Neumann, W. L.; Fanwick, P. E.; Janik, M.; Deutsch, E. A. Potential Gallium-68 Tracers for Imaging the Heart with Positron Emission Tomography: Evaluation of Four Ga-Complexes with Functionalized Tris(salicylaldimine) Ligands. *J. Nucl. Med.* **1993**, *34*, 228–233.

(6) Kung, H. F.; Liu, B. L.; Mankoff, D.; Kung, M. P.; Billings, J. J.; Francesconi, L.; Alavi, A. A New Myocardial Imaging Agent: Synthesis, Characterization, and Biodistribution of Gallium-68-BAT-TECH. *J. Nucl. Med.* **1990**, *31*, 1635–1640.

(7) Green, M. A.; Mathias, C. J.; Tsang, B. W.; Neumann, W. L.; Woulfe, S. R. Structure-Distribution Relationships for Gallium Tris(salicylaldimine) and Related Tris(aminophenol) Complexes. *J. Labelled Compds Radiopharm.* **1994**, *35*, 350–353.

(8) (a) Deutsch, E. Clinical PET: Its Time Has Come? *J. Nucl. Med.* **1993**, *34*, 1132. (b) Nunn, A. D. Single Photon Radiopharmaceuticals for Imaging Myocardial Perfusion. In *Radiopharmaceuticals: Chemistry and Pharmacology*; Nunn, A. D., Ed.; Marcel Dekker: New York, 1992; pp 97–140.

(9) (a) Kronauge, J. F.; Chiu, M. L.; Cone, J. S.; Davison, A.; Holman, B. L.; Jones, A. G.; Piwnica-Worms, D. Comparison of Neutral and Cationic Myocardial Perfusion Agents: Characteristics of Accumulation in Cultured Cells. *Nucl. Med. Biol.* **1992**, *19*, 141–148. (b) Jones, A. G.; Abrams, M. J.; Davison, A.; Brodack, J. W.; Toothaker, A. K.; Adelstein, S. J.; Kasis, A. I. Biological Studies of a New Class of Technetium Complexes: the Hexakis(alkylisonitrile)technetium(I) Cations. *Int. J. Nucl. Med. Biol.* **1984**, *11*, 225–234.

(10) Deutsch, E.; Ketring, A. R.; Libson, K.; Vanderheyden, J.-L.; Hirth, W. W. The Noah's Ark Experiment: Species Dependent Biodistributions of Cationic ^{99m}Tc Complexes. *Nucl. Med. Biol.* **1989**, *16*, 191–232.

(11) Tsang, B. W.; Mathias, C. J.; Green, M. A. A Gallium-68 Radiopharmaceutical That is Retained in Myocardium: ^{68}Ga-[(4,6-(MeO)$_2$sal)$_2$BAPEN]$^+$. *J. Nucl. Med.* **1993**, *34*, 1127–1131.

(12) DasSarma, B.; Bailar, J. C. The Stereochemistry of Metal Chelates with Polydentate Ligands Part I. *J. Am. Chem. Soc.* **1955**, *77*, 5476.

(13) Das Sarma, B.; Ray, K. R.; Sievers, R. E.; Bailar, J. C. The Stereochemistry of Metal Chelates with Multidentate Ligands Part II. *J. Am. Chem. Soc.* **1964**, *86*, 14–16.

(14) Green, M. A.; Welch, M. J.; Huffman, J. C. Synthesis and crystallographic characterization of a gallium salicylaldimine complex of radiopharmaceutical interest. *J. Am. Chem. Soc.* **1984**, *106*, 3689–3691.

(15) Sinn, E.; Sim, G.; Dose, E. V.; Tweedle, M. F.; Wilson, L. J. Electronic and molecular structure of variable-spin Fe(III) chelates with hexadentate ligands derived from triethylenetetramine and β-diketones or salicylaldehyde. *J. Am. Chem. Soc.* **1978**, *100*, 3375–3390.

(16) A reviewer has questioned whether the 5–10% propylene glycol included in these ^{67}Ga radiopharmaceutical preparations might alter their biodistribution. While propylene glycol is widely used as a pharmaceutical excipient, intravenous administration can produce cardiac effects.[17] To assess whether the propylene glycol excipient in our studies might have altered tracer uptake in the heart by changing the rate of myocardial blood flow, we have determined the biodistribution of the perfusion tracer [^{67}Cu]-PTSM[18] when administered in either 0.2 mL of 5% ethanol/95% saline or 0.2 mL of 5% ethanol/10% propylene glycol/85% saline. The addition of 10% propylene glycol to the injectate was found to have no effect on [^{67}Cu]PTSM biodistribution under conditions identical to those employed with the ^{67}Ga tracers reported herein. Thus, we conclude that ~0.02 mL of propylene glycol in the iv injectate has no substantial effect on myocardial (or cerebral) blood flow and is unlikely to have altered the biodistribution of the ^{67}Ga agents. The [^{67}Cu]PTSM biodistribution data are included in the supplementary material.

(17) Smolinske, S. C. *Handbook of Food, Drug, and Cosmetic Excipients*; CRC Press: Boca Raton, FL, 1992; pp 307–324.

(18) (a) John, E.; Green, M. A. Structure-Activity Relationships for Metal-Labeled Blood Flow Tracers: Comparison of Keto Aldehyde Bis(thiosemicarbazonato)copper(II) Derivatives. *J. Med. Chem.* **1990**, *33*, 1764–1770. (b) Green, M. A.; Mathias, C. J.; Welch, M. J.; McGuire, A. H.; Perry, D.; Fernandez-Rubio, F.; Perlmutter, J. S.; Raichle, M. E.; Bergmann, S. R. ^{62}Cu-Labeled Pyruvaldehyde Bis(N^4-methylthiosemicarbazonato)copper(II): Synthesis and Evaluation as a Positron Emission Tomography Tracer for Cerebral and Myocardial Perfusion. *J. Nucl. Med.* **1990**, *31*, 1989–1996. (c) Herrero, P.; Markham, J.; Weinheimer, C. J.; Anderson, C. J.; Welch, M. J.; Green, M. A.; Bergmann, S. R. Quantification of Regional Myocardial Perfusion with Generator-Produced ^{62}Cu-PTSM and Positron Emission Tomography. *Circulation* **1993**, *87*, 173–183.

(19) Barefield, E. K.; Wagner, F.; Herlinger, A. W.; Dahl, A. R. Preparation of (1,4,8,11-tetraazacyclotetradecane)nickel(II) Perchlorate and 1,4,8,11-Tetraazacyclotetradecane. *Inorg. Synth.* **1976**, *16*, 220–225.

(20) Kerr, J. M.; Suckling, C. J.; Bamfield, P. Selective Functionalisation. Part II. Selective Hydrogenation by a Novel Salicylideneethylenediamine Complex and the Properties of Derivatives of Some Square Planar Homogeneous Hydrogenation Catalysts. *J. Chem. Soc., Perkins Trans. I* **1990**, 887–895.

(21) (a) Sargent, M. V.; Stransky, P. O. Naturally Occurring Dibenzofurans. The Synthesis of Schizopeltic Acid. *J. Chem. Soc., Perkin Trans. I* **1982**, 2372. (b) Mali, R. S.; Yadav, V. J.; Zaware, R. N. An Improved Synthesis of Naturally Occurring Coumarins: Synthesis of Herniarin, Scoparone and 7-Methoxy-6-methyl Coumarin. *Indian J. Chem.* **1982**, *21B*, 759–760.

(22) Physical data for tris(salicylaldimines). (a) Physical data for (sal)$_3$BAPEN: mp 78–79 °C; FAB-MS for $C_{29}H_{34}N_4O_3$ shows a $[M + H]^+$ peak at 487 *m/z*; FTIR (KBr pellet): ν(C=N) 1636 cm^{-1}; ^{1}H-NMR ($CDCl_3$, TMS) δ 1.84 (m, 4H), 2.33 (m, 2H), 2.60 (m, 4H), 3.46 (m, 4H), 3.67 (m, 2H, CH_2), 3.63 (s, 1H, NCHN), 7.00 (m, 12H, ØH), 8.13 (s, 2H, CH=N). (b) Physical data for (5-MeOsal)$_3$BAPEN: mp 89–90 °C; FAB-MS for $C_{32}H_{40}N_4O_6$ shows $[M + H]^+$ peak at 577 *m/z*; FTIR (KBr pellet): ν(C=N) 1635 cm^{-1}; ^{1}H-NMR ($CDCl_3$, TMS) δ 1.86 (m, 4H), 2.71 (m, 8H), 3.70 (m, 4H, CH_2), 3.77 (m, 9H, OCH_3), 3.79 (s, 1H, NCHN), 6.70–6.94 (m, 9H, ØH), 8.30 (s, 2H, CH=N). (c) Physical data for (4-MeOsal)$_3$BAPEN: oil; FAB-MS for $C_{32}H_{40}N_4O_6$ shows $[M + H]^+$ peak at 577 *m/z*; FTIR (KBr pellet): ν(C=N) 1634 cm^{-1}; ^{1}H-NMR ($CDCl_3$, TMS) δ 1.81 (m, 4H), 2.28 (m, 2H), 2.50 (m, 2H), 2.67 (m, 4H), 3.58 (m, 2H), 3.41 (m, 2H, CH_2), 3.70 (s, 3H), 3.80 (s, 6H, OCH_3), 3.81 (s, 1H, NCHN), 6.21–6.42 (m, 6H), 6.77–7.10 (m, 3H, ØH), 8.14 (m, 2H, CH=N). (d) Physical data for (4-MeO-6-Mesal)$_3$BAPEN: oil; FAB-MS for $C_{35}H_{46}N_4O_6$ shows $[M + H]^+$ peak at 618 *m/z*; ^{1}H-NMR ($CDCl_3$, TMS) δ 1.81 (m, 4H), 1.98 (m, 2H, CH_2N), 2.20 (s, 3H), 2.32 (s, 6H, CH_3), 2.36 (m, 2H), 2.53 (m, 2H), 2.64 (m, 2H), 3.40 (m, 2H), 3.68 (m, 2H, CH_2), 3.65 (s, 3H, OCH_3), 3.77 (s, 6H, OCH_3), 4.06 (s, 1H, NCHN), 6.13 (m, 6H, ØH), 8.26 (s, 2H, CH=N). (e) Physical data for (4-MeO-5-Mesal)$_3$BAPEN: mp 149–150 °C; FAB-MS for $C_{35}H_{46}N_4O_6$ shows $[M + H]^+$ peak at 618 *m/z*; ^{1}H-NMR ($CDCl_3$,-TMS) δ 1.78 (m, 4H, CH_2N), 1.98 (s, 3H, CH_3), 2.10 (s, 6H, CH_3), 2.26 (m, 2H), 2.48 (m, 2H), 2.63 (m, 2H), 3.31 (m, 2H), 3.41 (m, 2H), 3.58 (m, 2H, CH_2), 3.52 (s, 1H, NCHN), 3.77 (s, 3H, OCH_3), 3.81 (s, 6H, OCH_3), 6.29–6.74 (m, 6H, ØH), 7.72 (s, 2H, CH=N). (f) Physical data for (4-EtO-6-Mesal)$_3$BAPEN: mp 76–77 °C; FAB-MS for $C_{38}H_{52}N_4O_9$ shows $[M + H]^+$ peak at 661 *m/z*; ^{1}H-NMR ($CDCl_3$, TMS) δ 1.38 (m, 9H, CCH_3), 1.80 (m, 4H), 1.98 (m, 2H, CH_2), 2.19 (s, 3H), 2.31 (s, 6H, $ØCH_3$), 2.36 (m, 2H), 2.53 (m, 2H), 2.64 (m, 2H), 3.39 (m, 2H), 3.66 (m, 2H, CH_2), 3.98 (m, 6H, OCH_2), 4.00 (s, 1H, NCHN), 6.13 (m, 6H, ØH), 8.24 (s, 2H, CH=N). (g) Physical data for (5-*i*-Prsal)$_3$-BAPEN: oil; FAB-MS for $C_{38}H_{52}N_4O_3$ shows $[M + H]^+$ peak at 612 *m/z*; ^{1}H-NMR ($CDCl_3$, TMS) δ 1.15 (m, 18H, CH_3), 1.75 (m, 4H), 2.24 (m, 2H), 2.45 (m, 2H), 2.68 (m, 2H), 3.52 (m, 6H, CH_2), 2.75 (m, 3H, ØCH), 3.39 (s,1H, NCHN), 6.00–6.19 (m, 6H), 6.70–7.20 (m, 9H, ØH), 8.32 (s, 2H, CH=N). (h) Physical data for (4-deasal)$_3$BAPEN: oil; FAB-MS for $C_{41}H_{61}N_7O_3$ shows $[M + H]^+$ peak at 700 *m/z*; FTIR (KBr pellet): ν(C=N) 1621 cm^{-1}; ^{1}H-NMR ($CDCl_3$, TMS) δ 1.22 (m, 18H, CH_3), 1.75 (m, 4H), 2.24 (m, 2H), 2.45 (m, 2H), 2.68 (m, 2H), 3.52 (m, 6H, CH_2), 3.40 (m, 12H, $ØNCH_2$), 3.49 (s, 1H, NCHN), 6.00–6.19 (m, 6H), 6.70–6.90 (m, 3H, ØH), 7.67 (m, 2H, CH=N). (i) Physical data for (4-deasal)$_3$Me$_4$BAPEN: oil; FAB-MS for $C_{45}H_{69}N_7O_3$ shows $[M + H]^+$ peak at 756 *m/z*; FTIR (KBr pellet): ν(C=N) 1624 cm^{-1}; ^{1}H-NMR ($CDCl_3$, TMS) δ 0.93 (s, 12H, CH_3), 1.16 (m, 18H, CH_3), 2.18 - 2.93 (m, 8H, CH_2), 3.26–3.43 (m, 17H, CH_2, NCHN), 5.99–6.96 (m, 9H, C_6H_3), 7.80 (m, 2H, CH=N).

(23) Physical data for GaL^+ complexes. (a) Physical data for Ga(sal)$_2$BAPEN$^+$I$^-$: FAB-MS for $C_{22}H_{26}N_4O_2Ga$ shows M^+ peak at 449 *m/z*; FTIR (KBr pellet): ν(C=N) 1630 cm^{-1}; ^{1}H-NMR (DMSO-d_6, TMS) δ 1.62 (m, 4H), 2.00 (m, 2H), 2.68 (m, 4H), 3.05 (m, 4H), 3.29, 3.45, 3.76 (m, 2H, CH_2), 5.15 (br s, 2H, NH), 7.28, 6.78 (m, 8H, C_6H_4), 8.31 (s, 2H, CH=N). (b) Physical data for Ga(5-MeO-sal)$_2$BAPEN$^+$I$^-$: FAB-MS for $C_{24}H_{32}N_4O_4Ga$ shows M^+ peak at 509 *m/z*; FTIR (KBr pellet): ν(C=N) 1631cm^{-1}; ^{1}H-NMR (DMSO-d_6, TMS) δ 1.58, 2.00, 2.66, 3.00, 3.28, 3.43, 3.75 (m, 16H, CH2), 3.67 (s, 6H, OCH_3), 5.10 (br s, 2H, NH), 7.05, 6.82 (m, 6H, ØH), 8.27 (s, 2H, CH=N). (c) Physical data for Ga(4-MeOsal)$_2$BAPEN$^+$I$^-$: FAB-MS for $C_{24}H_{32}N_4O_4Ga$ shows M^+ peak at 509 *m/z*; FTIR (KBr pellet): ν(C=N) 1625 cm^{-1}; ^{1}H-NMR (DMSO-d_6, TMS) δ 1.58, 1.99, 2.66, 2.99, 3.20, 3.46, 3.79 (m, 14H, CH_2), 3.78 (s, 6H, OCH_3), 5.08 (br s, 2H, NH), 6.32 (m, 4H), 7.18 (m, 2H, ØH), 8.15 (m, 2H, CH=N). (d) Physical data for Ga(4-MeO-6-Mesal)$_2$BAPEN$^+$I$^-$: mp >298 °C dec; FAB-MS for $C_{26}H_{36}N_4O_4Ga$ shows M^+ peak at 537 *m/z*; ^{1}H-NMR (DMSO-d_6, TMS) δ 1.58 (m, 2H), 1.98 (m, 2H, CH_2), 2.22 (s, 6H, $ØCH_3$), 2.66 (m, 2H), 2.97 (m, 4H), 3.32 (m, 2H), 3.41 (m, 2H), 3.70 (m, 2H, CH_2), 3.75 (s, 6H, $ØOCH_3$), 4.96 (br, 2H, NH), 6.16 (m, 4H, ØH), 8.28 (s, 2H, CH=N). (e) Physical data for Ga(4-MeO-5-Mesal)$_2$BAPEN$^+$I$^-$: FAB-MS for $C_{26}H_{36}N_4O_4Ga$ shows M^+ peak at 537 *m/z*; ^{1}H-NMR (DMSO-d_6, TMS) δ 1.55 (m, 2H), 1.96 (m, 2H, CH_2); 2.00 (s, 6H, $ØCH_3$), 2.66 (m, 2H), 2.98 (m, 4H), 3.19 (m, 2H), 3.47 (m, 2H), 3.77 (m, 2H, CH_2), 3.81 (s, 6H, $ØOCH_3$), 5.03 (br, 2H, NH), 6.33 (s, 2H), 6.96 (s, 2H, ØH), 8.07 (s, 2H, CH=N). (f) Physical data for Ga(4-EtO-6-Mesal)$_2$BAPEN$^+$I$^-$; FAB-MS for $C_{28}H_{40}N_4O_4Ga$ shows M^+ peak at 565 *m/z*; ^{1}H-NMR (DMSO-d_6, TMS) δ 1.31 (t, 6H, CCH_3), 1.58 (m, 2H), 1.96 (m, 2H, CH_2), 2.21 (s, 6H, $ØCH_3$), 2.65 (m, 2H), 2.97 (m, 4H), 3.40 (m, 4H), 3.70 (m, 2H, CH_2), 4.05 (m, 4H, $ØOCH_2$), 4.96 (br, 2H, NH), 6.16 (m, 4H, ØH), 8.28 (s, 2H, CH=N). (g) Physical data for Ga(5-*i*-Prsal)$_2$BAPEN$^+$I$^-$: FAB-MS for $C_{28}H_{40}N_4O_2Ga$ shows M^+ peak at 533 *m/z*; ^{1}H-NMR (DMSO-d_6, TMS) δ 1.14 (m, 12H, CH_3), 1.58 (m, 2H), 1.97 (m, 2H), 2.65 (m, 2H), 2.76 (quin, 2H, ØCH), 2.98 (m, 4H), 3.24 (m, 2H), 3.43 (m, 2H), 3.75 (m, 2H, CH_2), 5.02 (br, 2H, NH), 7.27 (m, 2H), 7.10 (m, 2H), 6.77 (m, 2H, ØH), 8.28 (s, 2H, CH=N). (h) Physical data for Ga(4-deasal)$_2$BAPEN$^+$I$^-$: 64% yield; >285 °C dec; FAB-MS for $[C_{30}H_{46}N_6O_2Ga]^+$ shows M^+ peak at 591 *m/z*; FTIR (KBr pellet): ν(C=N) 1596 cm^{-1}; ^{1}H-NMR (500 MHz, DMSO-d_6, TMS) δ 1.53 (m, 2H), 1.92 (m, 2H), 2.63 (m, 2H), 2.92 (m, 4H), 3.11 (m, 2H), 3.40 (m, 2H), 3.83 (m, 2H, CH_2), 3.22 (m, 8H, $ØNCH_2$), 4.86 (br s, 2H, NH), 5.87 (m, 2H), 6.11 (m, 2H), 6.96 (m, 2H, ØH), 7.89 (s, 2H, CH=N). (i) Physical data for Ga(4-deasal)$_2$DM-BAPEN$^+$I$^-$: FAB-MS for $[C_{34}H_{54}N_6O_2Ga]^+$ shows M^+ peak at 647 *m/z*; ^{1}H-NMR (DMSO-d_6, TMS) δ 0.79, 0.91 (s, 12H, CH_3), 1.12 (m, 12H, $ØNCCH_3$), 3.37 (m, 8H, NCH_2C), 2.74, 3.31, 3.89 (m, 12H, CH_2), 4.56 (br s, 2H, NH), 5.87, 6.12, 6.98 (m, 6H, ØH), 7.77 (m, 2H, CH=N).

(24) Walker, N.; Stuart, D. An Empirical Method for Correcting Diffractometer Data for Absorption Effects. *Acta Crystallogr., Sect. A: Found. Crystallogr.* **1983**, *A39*, 158–165.

(25) Sheldrick, G. M. *SHELX-86. Programe for the Solution of Crystal Structures*; University of Gottingen: F.R.G., 1986.

(26) Killean, R. C. G.; Lawrence, J. L. Least-Squares Weighting Schemes for Diffractometer Collected Data. IV. The Effect of Random Errors in the Form Factors Resulting from Bonding. *Acta Crystallogr., Sect. B: Struct. Crystallogr. Cryst. Chem.* **1969**, *25*, 1750–1752.

(27) Cromer, D. T.; Waber, J. T. *International Tables for X-ray Crystallography;* The Kynoch Press: Birmingham, England, 1974, Vol. IV, Tables 2.2B and 2.3.1.

(28) Cruickshank, D. W. J. The Accuracy of Atomic Coordinates Derived by Least-Squares of Fourier Methods. *Acta Crystallogr.* **1949**, *2*, 154–157.

(29) Bates, R. G.; Vega, C. A.; White, D. R. Standards for pH Measurements in Isotonic Saline Media of Ionic Strength I=0.16. *Anal. Chem.* **1978**, *50*, 1295–1300.